AIAA JOURNAL
Vol. 48, No. 12, December 2010

Comparing Pure-Pitch and Pure-Plunge Kinematics for a Symmetric Airfoil

Sunetra Sarkar*
Indian Institute of Technology Madras, Chennai 600 036, India

DOI: 10.2514/1.J050103

A set of pure sinusoidal pitch and plunge oscillations for a symmetric airfoil is studied in this paper. A gridless Lagrangian vorticity particle-based solver is used to simulate the unsteady flowfield. Various kinematics chosen here are inspired by the experimental and computational studies presented in earlier works. The Lagrangian tool is used to accurately reproduce the flowfield obtained by earlier experimental results. It follows the experimental trend better compared with some of the grid-based solvers' results from earlier studies. The strength of this tool is its grid-free nature, as the resolution of the grid is a crucial parameter in resolving the unsteady flowfield accurately. This study also investigates the effects of the starting condition in dictating the wake deflection mode at short and long terms and confirms the findings of the earlier works. The effect of mean angle of attack on the wake deflection is also highlighted. One of the main questions considered here is whether there exists a kinematic equivalence between sinusoidal pitch and plunge. Effective angle of attack, quasi-steady criterion, and Theodorsen's criterion of unsteady aerodynamics have been considered here for kinematic equivalence with plunge. The latter two give a reasonably good match both in terms of flowfield and load as was also reported in the literature. This behavior is seen in two different plunge stroke amplitude cases studied here. The success of the quasi-steady and Theodorsen's approach indicates the general wake behavior being an inviscid phenomenon, at least for the chosen range of parameters.

Nomenclature

c	=	chord length, m
h	=	normalized instantaneous heave
h_0	=	normalized heave amplitude
k	=	reduced frequency ($\omega c/U_\infty$)
U_∞	=	freestream velocity, m/s
ω	=	frequency of oscillation, rad/s
τ	=	nondimensional time (tU_∞/c)
α_m	=	mean angle of attack
α_0	=	pitch amplitude
ψ	=	phase angle
ϕ	=	phase of the starting position
$\mathbf{\Omega}$	=	vorticity vector
$\mathbf{V}$	=	velocity vector
ν	=	kinematic viscosity

I. Introduction

A SET of pure pitching and pure plunging motions are investigated in this paper using a Lagrangian viscous vortex technique. These kinematics are fundamental to any flapping mechanism of a micro-aerial vehicle. This investigation is inspired by an earlier study of McGowan et al. [1] in which a comparison of experimental and computational fluid dynamics results (based on CFL3D and immersed boundary method) for pure-pitch and -plunge kinematics was taken up. A set of pure sinusoidal plunging and its kinematically equivalent pitching using the same reduced frequency and effective angle of attack were investigated. The comparisons were made in terms of flowfield visualization and downstream velocity profile as a measure of thrust in [1]. The pure-plunge case was taken from an experiment of Lai and Platzer [2]. The agreement between the experimental and computational results was excellent for the pure-plunge case. However, for the equivalent pure-pitch case, the wake structure showed deflection in experiments which was not present in the pure-plunge case. This deflection was not captured in the original computational investigation of McGowan et al. [1] using CFL3D and immersed boundary-based solver. We take up this anomaly first using our Lagrangian solver for different starting conditions. Lai and Platzer [2] reports the importance of starting conditions in deciding the mode of trailing wake deflection. A nonzero mean angle of attack was also chosen arbitrarily in [1] for comparison with the plunge case, whereas a valid comparison would need to have the same mean angle of attack for both plunge and pitch. In the present work, mean angle of attack is also varied for the pitch case to show how the wake deflection depends on the total angle of attack and not only the amplitude. The role of the starting condition in dictating the wake deflection mode is also studied for the different mean angle of attack cases.

In a subsequent work, Alam et al. [3] took up the same investigations comprehensively for longer time and with different starting conditions and obtained wake deflection by a different computational model based on Ansys CFX. There was also a second time scale much larger than the initial transient time. By the initial transients, wake deflection shows up and the mode of deflection depends on the starting conditions. However, all the wakes eventually (by the second time scale) looks to be upwardly deflected irrespective of the starting conditions. This second time scale could be as high as 20 cycles or more. This is an interesting observation and we also simulate the same here for a symmetric profile. The findings are quite similar even for the symmetric profile which is rather surprising as a symmetric profile need not have a directional bias.

McGowan et al. [4] further probes into the equivalence of plunge and pitch kinematics and looks for the best equivalent pitching kinematics which would match the plunge flowfield. This is based on both quasi-steady and Theodorsen criteria of unsteady aerodynamic theory. Our Lagrangian investigation confirms the findings, results are presented in brief. Though strictly speaking, for a viscous flowfield, it is not possible to find a kinematic equivalent pitch analytically. However, the wake deflection is primarily an inviscid phenomenon argued by Jones et al. [5].

In this work, the results are presented and compared with the earlier works in terms of vorticity fields during upstroke and downstroke and also in some cases in terms of streamwise velocity profiles and lift coefficients.

Presented as Paper 2009-3815 at the 39th AIAA Fluid Dynamics Conference, San Antonio, TX, 22 June–25 2009; received 28 July 2009; revision received 12 June 2010; accepted for publication 8 August 2010. Copyright © 2010 by the American Institute of Aeronautics and Astronautics, Inc. All rights reserved. Copies of this paper may be made for personal or internal use, on condition that the copier pay the $10.00 per-copy fee to the Copyright Clearance Center, Inc., 222 Rosewood Drive, Danvers, MA 01923; include the code 0001-1452/10 and $10.00 in correspondence with the CCC.

*Department of Aerospace Engineering; sunetra.sarkar@gmail.com.

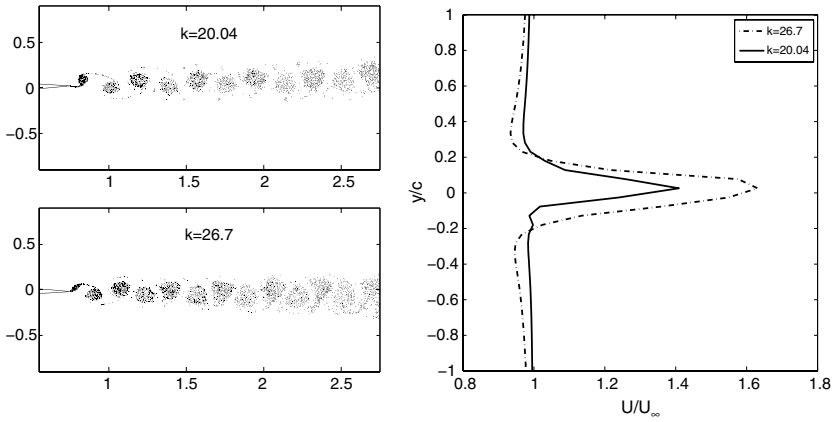

a) b)

Fig. 1 Experimental validation from Koochesfahani [16]; $k = 20.04, 26.7$: a) wake pattern and b) mean streamwise velocity profiles.

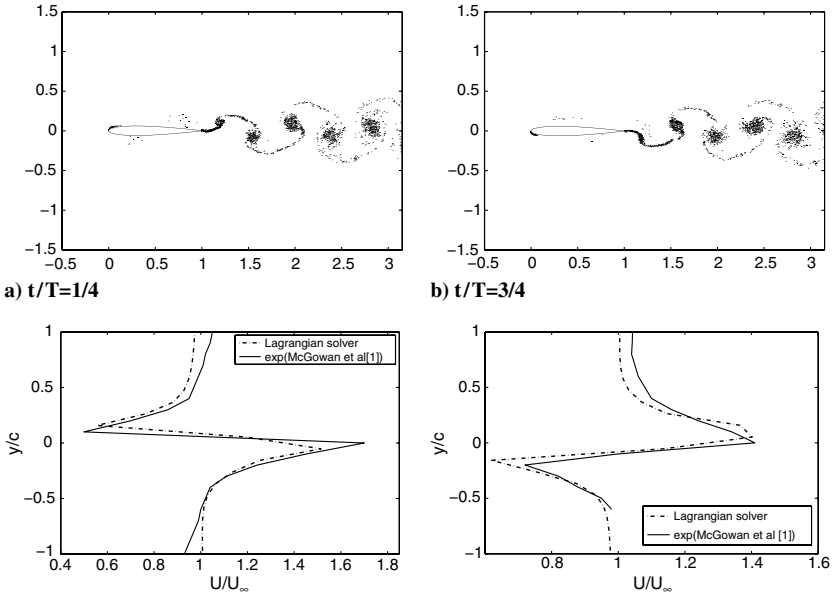

a) t/T=1/4 b) t/T=3/4

c) t/T=1/4 d) t/T=3/4

Fig. 2 Pure heave: vorticity plot and instantaneous streamwise velocity profile using Lagrangian viscous solver; $h_0 = 0.05, k = 7.86$.

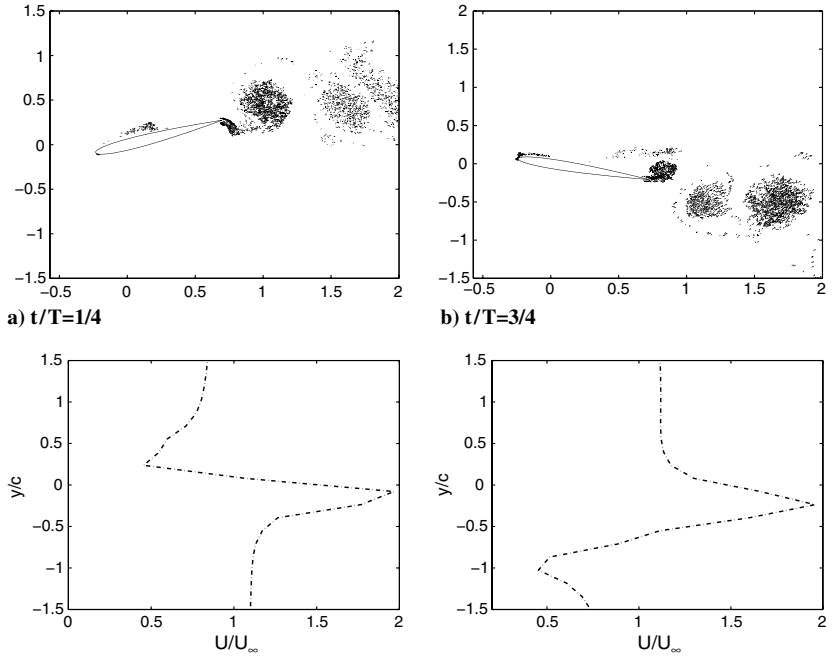

a) t/T=1/4 b) t/T=3/4

c) t/T=1/4 d) t/T=3/4

Fig. 3 Pure-pitch: vorticity plot and instantaneous streamwise velocity profile by Lagrangian viscous solver; $\alpha_0 = 21.5°, k = 7.86, \alpha_m = 0°$.

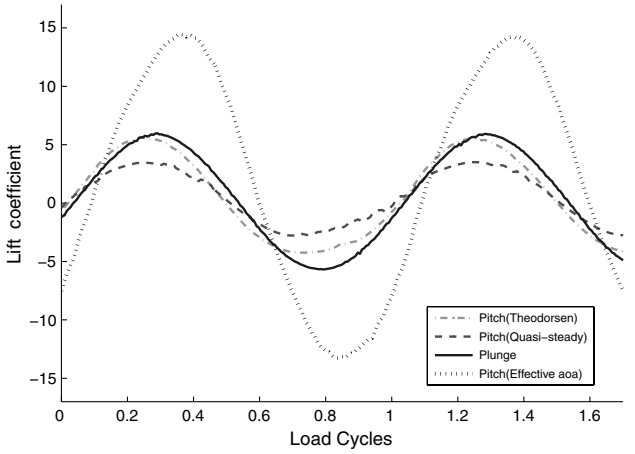

Fig. 4 Lift coefficient for plunge and equivalent pitch kinematics based on effective angle of attack, quasi-steady and Theodorsen's approach; $k = 7.86$, $\alpha_m = 0°$.

II. Lagrangian Solver

This is a grid-free technique and the flowfield is described by a number of discrete particles carrying field property vorticity. The incompressible Navier–Stokes equation is solved in terms of vorticity. Velocity field is computed from the Biot–Savart law, obtained from the vector Poisson equation of vorticity-stream function. Various diffusion models can be used in order to simulate viscous diffusion. In our work, a random walk model is used [6]. In some of our earlier works, this Lagrangian method was used to simulate the unsteady flowfield related to dynamic stall and heaving-propulsion [7,8].

The two-dimensional incompressible Navier–Stokes equation in the vorticity-transport form is shown as [9]

$$\frac{D\Omega}{Dt} = \nu\nabla^2\Omega \tag{1}$$

where ν is the kinematic viscosity, vorticity $\boldsymbol{\Omega} = \nabla \times \mathbf{V}$ with $\mathbf{V}$ the velocity field. The vorticity and the velocity field is given by a vector Poisson equation [9,10]:

$$\nabla^2\mathbf{V} = -\nabla \times \boldsymbol{\Omega} \tag{2}$$

The solution to this vector Poisson equation uniquely defines the velocity-vorticity relationship, known as the Biot–Savart law [9–11] as shown below:

$$\mathbf{V}(\mathbf{r}, t) = -\frac{1}{2\pi}\left[\int_R \frac{\boldsymbol{\Omega} \times (\mathbf{r}_0 - \mathbf{r})}{|\mathbf{r}_0 - \mathbf{r}|^2}\,\mathrm{d}R + 2\int_S \frac{\boldsymbol{\Omega}_b \times (\mathbf{r}_0 - \mathbf{r})}{|\mathbf{r}_0 - \mathbf{r}|^2}\,\mathrm{d}S + \mathbf{V}_\infty\right] \tag{3}$$

where $\boldsymbol{\Omega}_b$ is the rigid body angular velocity of the solid whose boundary is denoted by S, and $\mathbf{V}_\infty$ its translational velocity. $\mathbf{r}_0$ is the vector distance from the origin of the reference frame to the vortex particles in the fluid region R, and $\mathbf{r}$ is the point in the flowfield where the induced velocity due to these vortex particles are to be determined. Note that the velocity field automatically satisfies the far-field velocity boundary condition of the flow.

New vortices are created at the body boundary by satisfying the no-slip and no-penetration boundary conditions. We use a operator splitting technique proposed by Chorin [6] in which Eq. (1) can be split into convection and diffusion parts that are to be solved sequentially. This is represented as

$$\partial\Omega/\partial t + \mathbf{V}.\nabla\Omega = 0, \quad \text{and} \quad \partial\Omega/\partial t = \nu\nabla^2\Omega \tag{4}$$

The convection part in Eq. (4) shows the invariance of vorticity of the vortex particles as they move with the fluid. The convection velocity is the same as that given by the Biot–Savart law. The solution of the diffusion part in Eq. (4) is given by a Gaussian probability density function [9]. A random walk algorithm [6] is used to approximate diffusion [12,13]. Recently, Eldredge et al. [14] used a viscous vortex particle method with a deterministic diffusion model to study

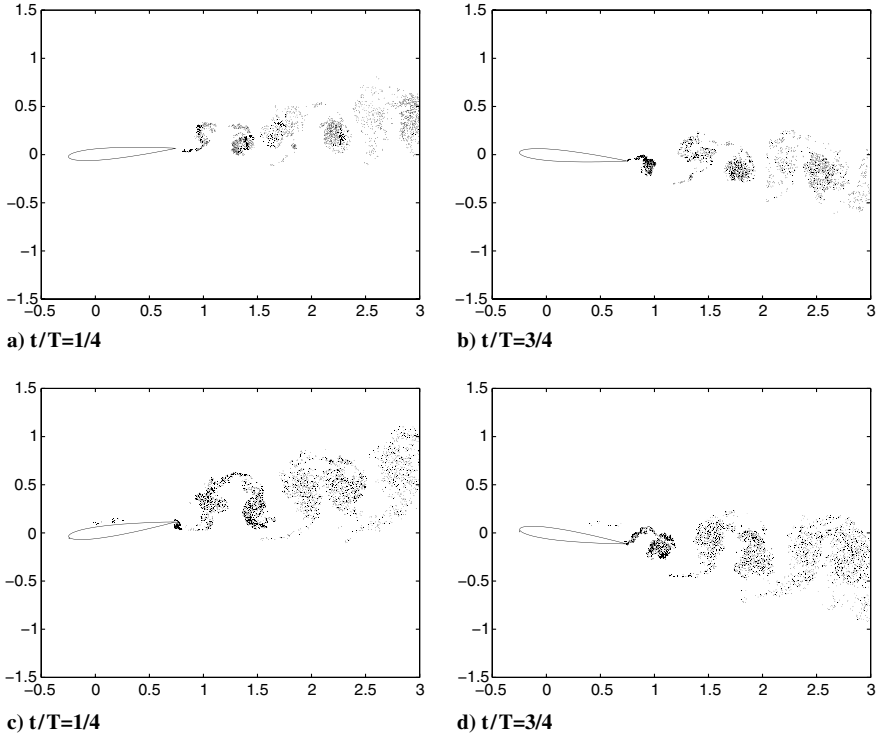

Fig. 5 Pure-pitch: a)–b) quasi-steady criterion $\alpha_0 = -5.6°$, $k = 7.86$, $\alpha_m = 0°$, $\psi = 14.3°$ and c)–d) Theodorsen's criterion $\alpha_0 = -8.9°$, $k = 7.86$, $\alpha_m = 0°$, $\psi = 35.8°$.

flapping kinematics of airfoils. In another investigation, Chabalko et al. [15] have used a vortex lattice method to study the pitch plunge kinematics of an airfoil.

The forces exerted on the body comes from the surface pressure and the surface friction. The tangential pressure gradient on the body surface is given by

$$\frac{1}{\rho}\frac{\partial p}{\partial \hat{s}} = -\hat{s}.\frac{D\mathbf{V}_b}{Dt} - \hat{n}.\mathbf{r}\frac{D\Omega_b}{Dt} + \hat{s}.\mathbf{r}\Omega_b^2 + \nu\frac{\partial \Omega}{\partial \hat{n}} \tag{5}$$

where Ω_b is the angular velocity of the body motion. Equation (5) is integrated to calculate the aerodynamic loads from the surface pressure distribution.

Some simple pure-pitch cases are simulated here with the above tool from Koochesfahani's [16] pitching experiments at $Re=10,000$. The trailing wake patterns and mean velocity profiles are shown in Fig. 1 and the results are encouraging. The k values shown here corresponds to frequencies 6 and 8 Hz as given in [16] and are based on full chord length. This solver can also capture strong viscous effects, for example, leading-edge dynamic stall vortex. For

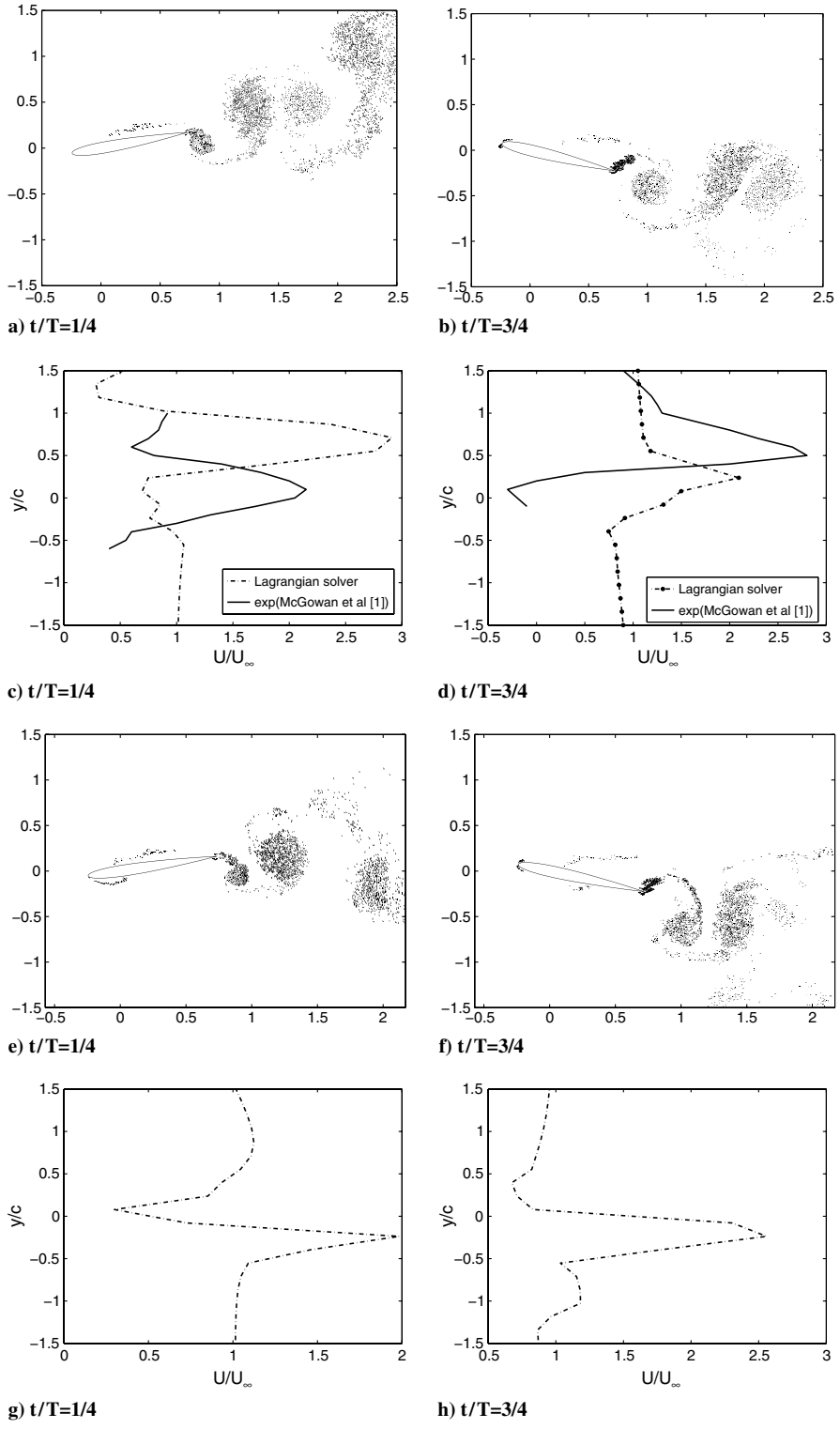

Fig. 6 Vorticity plot and instantaneous streamwise velocity profile for heave-equivalent pitch using effective angle of attack: a)–d) $\phi = \pi/2$ and e)–h) $\phi = 3\pi/2$; $\alpha_0 = 21.5°$, $k = 7.86$, $\alpha_m = 4°$.

experimental validation in such regimes, our earlier results in [7] can be referred to.

III. Flapping Kinematics

The nondimensional heaving kinematics is given by [2]

$$h(t) = h_0 \cos(k\tau) \tag{6}$$

Here, h and h_0 are the normalized (with the chord) heave and heave amplitude, respectively, $k = \omega c/U_\infty$ is the reduced frequency and $\tau = tU_\infty/c$ is the nondimensional time. An effective angle of attack-based pitching motion can be constructed from the heave [17] as: $\alpha(t) = \tan^{-1}[-\dot{h}_1/U_\infty]$. Here $h_1 = hc$ is the instantaneous heave in the dimensional form. The corresponding pitch amplitude would be: $\alpha_0 = \tan^{-1}[h_0 k]$. Thus a sinusoidal heave-equivalent pitch motion with a reduced frequency same as the heave and an arbitrary mean angle of attack α_m is given by

$$\alpha(t) = \alpha_m + \alpha_0 \cos(k\tau + \psi) \tag{7}$$

McGowan et al. [1] had chosen the following parameters from Lai and Platzer [2]: $h_0 = 0.05$, $k = 7.86$. Note that reduced frequency in [1] was described using the half-chord unlike in the present work or in [2] where chord-length is used for nondimensionalization. For the pure-pitch case, an arbitrary mean angle of attack of 4° was used in their study. Using these parameters, the pitching amplitude is calculated as $\alpha_0 = 21.5°$. Using quasi-steady theory and Theodorsen's theory of unsteady aerodynamics, alternate pitch amplitudes and phase angles are calculated in [4]. The difference between the quasi-steady theory and effective angle of attack approach is that the effect of pitch rate is included in the former. Theodorsen's approach includes the noncirculatory terms as well which are absent in the other two; it also includes the wake effect through a complex function of reduced frequency called Theodorsen's function. The pitch amplitudes and the phase angles are calculated as $\alpha_0 = -5.6°$, $\psi = 14.3°$ and $\alpha_0 = -8.9°$, $\psi = 35.8°$ by quasi-steady and Theodorsen's criteria, respectively. These derivations have been discussed in details in [4] and are not repeated here. Effects of two different Reynolds numbers (Re) of 10,000 and 40,000 were also compared in [1,3] but no significant difference in the results were observed. In the present study, Re is kept at 10,000.

In the present work, we use two different starting conditions, trailing edge going up and going down starting from the mean position. They have been referred to as the upward and downward starting conditions and are denoted by $\phi = \pi/2$ and $\phi = 3\pi/2$ respectively as per the notation used in [3].

IV. Results and Discussion

A symmetric NACA 0012 profile is chosen here; the Lagrangian viscous solver described in the earlier section is used for simulation. The Reynolds number is kept at 10,000 for all cases. First, pure heave kinematics is taken up (from Lai and Platzer [2]). The Lagrangian solver results are shown in Fig. 2 which closely match with that of Lai and Platzer [2]. The trace of leading-edge vortex is insignificant; the trailing-edge vortex pattern shows anticlockwise vortices in the upper row and clockwise vortices in the lower row. This vortex street which is opposite in sense of a Karman street indicates thrust.

The instantaneous values of the streamwise velocity profiles are plotted in Figs. 2c and 2d to compare with the experiments of McGowan et al. [1] and they match quite well. The streamwise velocity profiles are normalized by the freestream velocity and have been plotted for the upstroke and downstrokes. The velocity profiles are calculated at a distance $x/\text{chord} = 2$ in the wake, as was also done by McGowan et al. [1].

For the pitching case, we first choose the effective angle of attack approach. However, any comparison with plunge should be made at the same mean angle of attack. So here we choose a zero mean angle in pitch. The vorticity contours along with the instantaneous streamwise velocity plots are shown in Fig. 3. The wake does not show any significant deflection. The velocity profiles also look similar to plunge (shown in Figs. 2c and 2d) though the numerical values are different. However, if one compares the lift coefficient C_l as was done in [4], the difference between the plunge and effective angle of attack pitch case is significant as shown in Fig. 4. The load comparison also includes the pitch kinematics based on quasi-steady and Theodorsen's approach [4]. For $h_0 = 0.05$, $k = 7.86$, the equivalent pitch amplitudes and phase angles are calculated as −5.6, 14.3° and −8.9, 35.8° with quasi-steady and Theodorsen's criteria, respectively. The lift coefficient for Theodorsen's criteria is closest to that of pure-plunge which confirms the findings in [4], though the results were presented there for a nonzero mean angle of 4°. The wake patterns are shown in Fig. 5 with the quasi-steady and Theodorsen's approaches. The wake patterns are close to that of plunge, however, quasi-steady match is somewhat better than Theodorsen's.

Now, we increase the mean angle of attack to 4°. The phase of the vorticity snapshots in a cycle are mentioned in terms of t/T as before. Here, $t/T = 1/4$ means maximum nose-down position and $t/T = 3/4$ means maximum nose-up position of the airfoil. The starting condition is also mentioned in terms of ϕ as discussed in the earlier section. We see that the wake deflection is noticeable as shown in Figs. 6a and 6b. Instantaneous streamwise velocity profiles are also shown in Figs. 6c and 6d in order to compare them with the experimental results of McGowan et al. [1] and the match is poor. Though both studies indicate deflection in the wake, the deflection looks much stronger in the phase averaged vorticity contour images from the experimental study of [1]. However, in our case, the deflection is gradual [2] and the immediate first pair do not show any significant deflection. Moreover, it is not clear after how many cycles the velocity profiles should be compared. In our Lagrangian simulations, both upward and downward starting conditions are used and the wake is deflected accordingly, see Figs. 6e–6h also. Alam et al. [3] revisits the cases presented in McGowan et al. [1], with a SD7003 profile as in [1]. An Ansys CFX-based computational model is chosen which captures the wake deflection successfully now. A systematic study of four different starting conditions was done which dictate the deflection mode. Simulations were run for long time and there was evidence of a second time scale by which all wake types eventually go to upward deflection mode irrespective of their starting conditions. This happens typically between 10–20 cycles. Interestingly, our observations with a symmetric profile are also quite similar. We choose a typical case of downward starting conditions from the mean angle position (phase $3\pi/2$ in [3]) and simulate it for a longer time beyond 10 cycles. The final wake form indeed comes out from its downward deflection mode and starts to look upwardly deflected. The wake patterns at tenth cycle are shown in Fig. 7. This

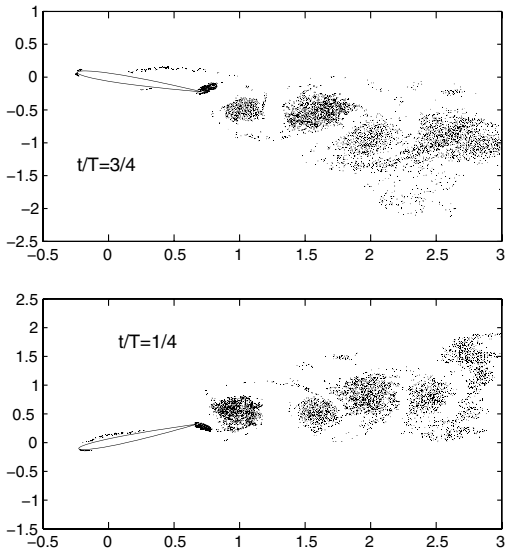

Fig. 7 Simulation of $\phi = 3\pi/2$ case from Fig. 6 [(e) and (f) cases] at the tenth cycle.

observation is counter intuitive and needs further investigations. A cambered profile can have preference for a particular deflection mode but a symmetric profile need not. Also, an upward deflected wake is also a signature of nonzero upward vertical force, which can happen in a cambered profile. Lai and Platzer [2] had mentioned the possibility of arbitrary changes in the deflection mode in their experiments which is supposedly triggered by small random disturbances present during the experiments. It will be worthwhile to see if any further changes of the deflection mode is possible, at least for the symmetric profile. However, at very long time, the Lagrangian tool will accumulate too many vortex particles slowing down the time marching process.

For a mean angle of attack of 8°, the immediate wake deflection is again dictated by the starting conditions. The deflection is much higher than the earlier case, the mushroom vortex shapes are visible as shown in Fig. 8. This also shows that the wake deflection is dependent on the total angle of attack and not the amplitude alone. The instantaneous streamwise velocity profiles are shown once again as in the earlier cases.

It is well known that the wake deflection in plunge is a function of its nondimensional plunge velocity, kh_0. Typically for $kh_0 = 1$ or more the wake of a plunging airfoil deflects [5]. The starting condition decides the mode of deflection, at least in the short time scale. In our earlier study on nonsinusoidal plunge [8], the wake

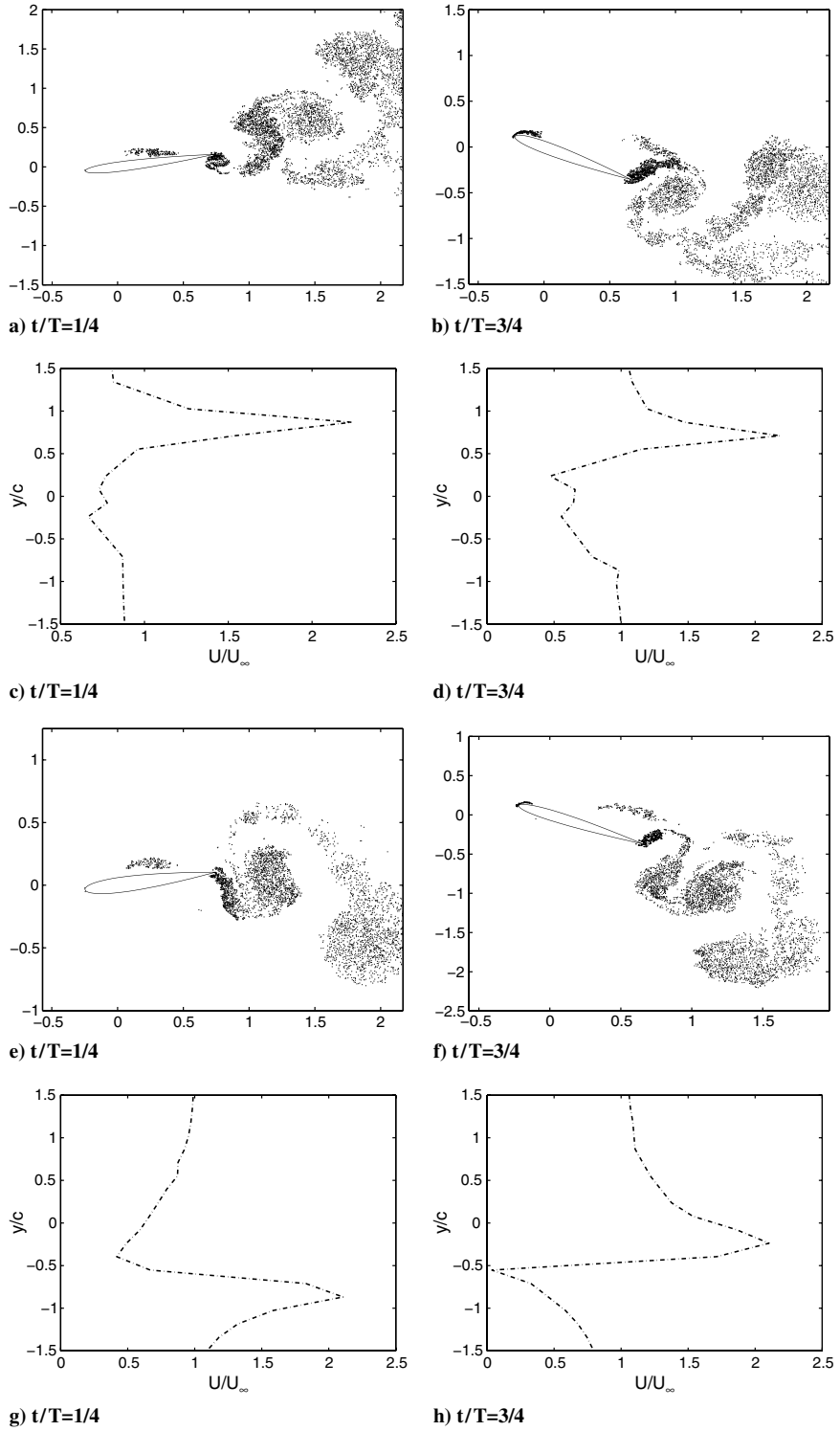

Fig. 8 Vorticity plot and instantaneous streamwise velocity profiles: a)–d) $\phi = \pi/2$ and e)–h) $\phi = 3\pi/2$; $\alpha_0 = 21.5°$, $k = 7.86$, $\alpha_m = 8°$.

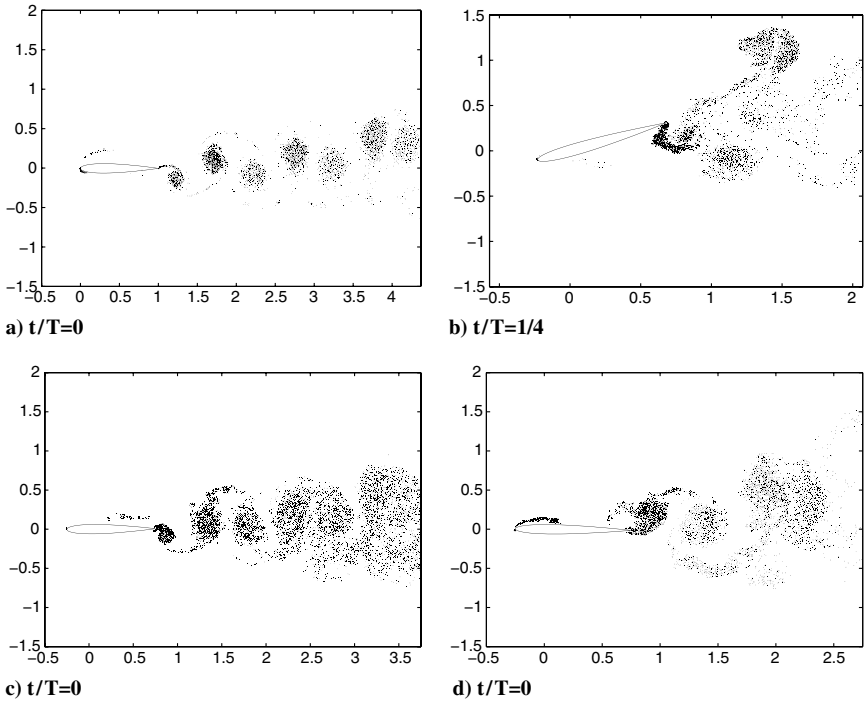

Fig. 9 Vorticity patterns for equivalent plunge $kh_0 = 1.0$ with $\phi = \pi/2$: a) pure-plunge, b) pure-pitch based on effective angle of attack $\alpha_0 = 44.5°$, $k = 7.86$, $\alpha_m = 0°$, $\psi = 90°$, c) quasi-steady criteria $\alpha_0 = -14.13°$, $k = 7.86$, $\alpha_m = 0°$, $\psi = 14.3°$, and d) Theodorsen's criteria $\alpha_0 = -22.54°$, $k = 7.86$, $\alpha_m = 0°$, $\psi = 35.8°$.

deflection was shown to be dependent on the starting condition. Lai and Platzer [2] shows the same for a sinusoidal plunge. Thus, both the pitch and plunge cases behave quite similarly. We also simulate a higher $kh_0 = 1$ case here. This is achieved by using a higher plunge amplitude $h_0 = 0.12$ and the same k as before. The corresponding pitch amplitude using the effective angle of attack criterion is 44.5° which is rather high. Mean angle is kept zero in pitch. The vortex pattern for the plunging case is shown in Fig. 9a for an upward starting condition. The effective angle of attack-based pitching case is shown in Fig. 9b. This wake pattern looks completely different; it shows a large upward deflection along with a smaller downward pattern. Equivalent pitch is also taken up using quasi-steady and Theodorsen's criteria. The corresponding pitch amplitudes and phase angles are, $\alpha_0 = -14.13°$, $\psi = 14.3°$ and $\alpha_0 = -22.54°$, $\psi = 35.8°$ respectively. The vorticity plots for these cases are shown in Figs. 9c and 9d. The wake pattern from the quasi-steady approach is quite close to that of plunge, same as in the earlier smaller kh_0 case. Theodorsen's approach shows a higher wake deflection than that of the quasi-steady approach. However, it would be interesting to see at what regime of Reynolds numbers this equivalence is lost, especially when the viscous effects are really high and strong leading-edge vortices are present.

V. Conclusions

This work simulates the unsteady flowfields for a set of pure-plunge and pure-pitch kinematics for a symmetric airfoil with a particle-based Lagrangian viscous solver. This tool can provide a quick visualization of the flow in terms of its vorticity. It has successfully captured the wake deflection seen in the pitching experiments of McGowan et al. [1]. However, the authors had also used two computational models (using grid-based CFL3D and immersed boundary method-based solvers) to simulate the same kinematics but wake deflection was absent. There is no special feature in the Lagrangian tool (other than this being grid-free) that could enable it to capture the unsteady flow field better compared with a grid-based solver. So, a possible reason for this mismatch could be insufficient grid resolution used in the grid-based solvers. Also, the starting condition plays a role in dictating the time required for obtaining the correct wake pattern after overcoming the transients. This is also called short-term stationarity which was analyzed in a later study quite systematically [3]. The evolution of both short-term and long-term stationarity were presented using an Ansys CFX solver with and without turbulence modeling. Both the time scales (short and long) were shown to vary with the starting conditions. As per our observations, the Lagrangian solver quickly converges to the short-term stationarity; for any starting condition the corresponding short-term stationarity is always reached within two to three cycles and the results are plotted around fifth/sixth cycle. An interesting question is, can arbitrary perturbations trigger the preferred mode of deflection. This could be the case for the present random vortex technique, at least for the short-term case. This, however, can not be a universal argument, until a comprehensive comparison is done.

The present Lagrangian code is not a very good choice to track the flow field at large time as the flow field becomes too crowded and the time marching becomes slow. A fast particle algorithm is needed. Here, the long-term behavior was investigated only for one starting condition. The long-term stationarity converges to an upward deflection mode for the symmetric airfoil which is surprising and needs further investigation. A symmetric profile need not have a bias for any preferred mode of deflection. Moreover, it remains to be seen if the long-term deflection mode can alter further at a later time with arbitrary perturbations.

The present study confirms the findings of McGowan et al. [4] that the quasi-steady criterion and Theodorsen's criterion of unsteady aerodynamics for choosing the kinematic equivalent pitch give a close match with plunge, both in terms of flowfield and load. This was done also for a higher stroke amplitude case with $kh_0 = 1.0$ and the findings were the same. $kh_0 = 1.0$ for plunge gives a slightly deflected wake as per Jones et al. [5] criteria. Quasi-steady and Theodorsen's theory work well, possibly because wake deflection seems to be essentially an inviscid phenomenon [5]. However, it remains to be seen in which regime the overall equivalence will be lost, especially when the viscous effects are much more significant.

Acknowledgments

Financial support for this work was given by Air Force Office of Scientific Research's Asian Office of Aerospace Research and

Development. We are also thankful to Michael V. Ol of Air Force Research Laboratory for bringing our attention to this problem.

References

[1] McGowan, G. Z., Gopalarathnam, A., Ol, M. V., Edwards, J. R., and Fredberg, D., "Computation vs Experiment for High-Frequency Low-Reynolds Number Airfoil Pitch and Plunge," AIAA Paper 2008-653, Jan. 2008.

[2] Lai, J. C. S., and Platzer, M. F., "Jet Characteristics of a Plunging Airfoil," *AIAA Journal*, Vol. 37, No. 12, 1999, pp. 1529–1537. doi:10.2514/2.641

[3] Alam, M., Suzen, Y. B., and Ol, M. V., "Numerical Simulation of Pitching Airfoil Flowfields for MAV Applications," AIAA Paper 2009-4029, June 2009.

[4] McGowan, G. Z., Gopalarathnam, A., Ol, M. V., and Edwards, J. R., "Analytical, Computational, and Experimental Investigations of Equivalence Between Pitch and Plunge Motions for Airfoil at Low Reynolds Numbers," AIAA Paper 2009-535, Jan. 2009.

[5] Jones, K., Dohring, C., and Platzer, M., "Experimental and Computational Investigation of the Knoller-Betz Effect," *AIAA Journal*, Vol. 36, No. 7, 1998, pp. 1240–1246. doi:10.2514/2.505

[6] Chorin, A., "Numerical Study of Slightly Viscous Flow," *Journal of Fluid Mechanics*, Vol. 57, No. 4, 1973, pp. 785–796. doi:10.1017/S0022112073002016

[7] Sarkar, S., and Venkatraman, K., "Influence of Pitching Angle of Incidence on the Dynamic Stall Behavior of a Symmetric Airfoil," *European Journal of Mechanics B: Fluids*, Vol. 27, No. 3, 2008, pp. 219–238. doi:10.1016/j.euromechflu.2006.07.004

[8] Sarkar, S., and Venkatraman, K., "Numerical Simulation of Incompressible Viscous Flow past a Heaving Airfoil," *International Journal of Numerical Methods in Fluids*, Vol. 51, No. 1, 2006, pp. 1–29. doi:10.1002/fld.1094

[9] Batchelor, G., *An Introduction to Fluid Dynamics*, Cambridge Univ. Press, New Delhi, India, 1967.

[10] Wu, J., and Thompson, J., "Numerical Solutions of Time-Dependent Incompressible Navier–Stokes Equations Using an Integro-Differential Formulation," *Computers and Fluids*, Vol. 1, No. 2, 1973, pp. 197–215. doi:10.1016/0045-7930(73)90018-2

[11] Lin, H., Vezza, M., and Galbraith, R. A. McD., "Discrete Vortex Method for Simulating Unsteady Flow Around Pitching Aerofoils," *AIAA Journal*, Vol. 35, No. 3, 1997, pp. 494–499. doi:10.2514/2.122

[12] Fogelson, A., and Dillon, R., "Optimal Smoothing in Function-Transport Particle Methods for Diffusion Problems," *Journal of Computational Physics*, Vol. 109, No. 2, 1993, pp. 155–163. doi:10.1006/jcph.1993.1208

[13] Fishelov, D., "A New Vortex Scheme for Viscous Flows," *Journal of Computational Physics*, Vol. 86, No. 1, 1990, pp. 211–224. doi:10.1016/0021-9991(90)90098-L

[14] Eldredge, J. D., Wang, C., and Ol, M. V., "A Computational Study of a Canonical Pitch-Up, Pitch-Down Wing Maneuver," AIAA Paper 2009-3687, June 2009.

[15] Chabalko, C. C., Snyder, R. D., Beran, P. S., and Ol, M. V., "Study of Deflected Wake Phenomena by 2D Unsteady Vortex Lattice," AIAA Paper 2009-2475, 2009.

[16] Koochesfahani, M., "Vortical Patterns in the Wake of an Oscillating Airfoil," *AIAA Journal*, Vol. 27, No. 9, 1989, pp. 1200–1205. doi:10.2514/3.10246

[17] McCroskey, W. J., "The Phenomenon of Dynamic Stall," NASA TM-81264, 1981.

P. Beran
Associate Editor